Formation of a Co nanostructure revealed by ^{59}Co nuclear magnetic resonance measurements in Co/Au multilayers

M. Wojcik
Institute of Physics, Polish Academy of Sciences, 02-668 Warsaw, Poland

C. Christides
Department of Engineering Sciences, School of Engineering, University of Patras, 26110 Patras, Greece

E. Jedryka and S. Nadolski
Institute of Physics, Polish Academy of Sciences, 02-668 Warsaw, Poland

I. Panagiotopoulos
Institute of Materials Science, NCSR ''Demokritos,'' 153 10 Aghia Paraskevi, Attiki, Greece
(Received 10 December 1999; revised manuscript received 11 February 2000; published 11 December 2000)

The effect of annealing on the microstructure of sputter-grown Co/Au multilayers with (111) texture is studied by means of x-ray diffraction (XRD) and spin-echo ^{59}Co nuclear magnetic resonance (NMR) spectroscopy. Both XRD and NMR spectra exhibit drastic changes after annealing at 350 °C, revealing a transformation from Co layering in the as-made multilayers to the known close-packed phases of Co. The thermal stability of the as-made Co layering up to 350 °C is assigned to a kinetically grown Co nanostructure.

DOI: 10.1103/PhysRevB.63.012102 PACS number(s): 75.70.−i, 76.60.Lz

Rapidly quenched $Co_{1-x}Au_x$ films[1] form a typical phase separation system, which can be a reference for the study of amorphous-crystalline transformations after annealing. According to the so-called Ostwald rule,[1] heat treatment of quenched $Co_{1-x}Au_x$ films produces transformations from the less stable state, with increased Au-Co atomic solubility in amorphous or single-phase metastable matrices, to a two-phase equilibrium fcc state through a succession of intermediate metastable phases of increasing stability. Thus, heating of amorphous Co-30Au films[1] above 150 °C resulted in irreversible change from the amorphous structure to a single metastable fcc crystalline structure, which subsequently decomposed into equilibrium Au and Co fcc structures above 300 °C. Practically it is important that annealing of Co-Au thin films or monolayers (ML's) required[1–3] only 10–60 min to complete structural transformations between 200 and 300 °C, whereas in bulk $Co_{1-x}Au_x$ alloys the microstructural changes continue as a function of aging time[4,5] up to a few days.

Currently, this phase separation process is applied to the cosputtered[2] $Co_{1-x}Au_x$ thin films or rapidly quenched ribbons[4] to engineer their magnetotransport properties after annealing. Heat treatment of Co/Au ML's at 300 °C revealed[3] a controllable way, with profound technological impact on magnetic-storage applications, to change the magnetic anisotropy of Co by sharpening the Co/Au interfaces. To the best of our knowledge, the observed structural transformations in the Co-Au phase diagram of $Co_{1-x}Au_x$ thin films,[1,2] multilayers,[3] and rapidly quenched ribbons[4,5] have been identified by standard x-ray scattering and electron microscopy techniques, but not with spin-echo ^{59}Co nuclear magnetic resonance (NMR) measurements.

Recently, low-field giant-magnetoresistance (GMR) was achieved in sputter-grown[6,7] Co/Au ML's after modification of the Co layering.[8,9] Investigation of the as-made $[Co(1\ nm)/Au(2.5\ nm)]_{30}$ ML's, which exhibit the maximum[7] GMR effect, with conventional and high-resolution transmission electron microscopy (TEM) has shown[9] that the Co layer structure adopts mainly an expanded fcc lattice. These measurements show that the Co lattice is expanded by 4.4% relative to the known close-packed Co. Also, ^{59}Co NMR spectra of the as-made ML's have revealed[8] a unique profile that could not be assigned to any of the known bulk crystalline or glassy Co structures. In this study our intent is to investigate the effect of post-annealing on the microstructure of the as-made $[Co(1\ nm)/Au(2.5\ nm)]_{30}$ ML's, using ^{59}Co NMR measurements as the microscopic technique.

Six separate ML's of $[Co(1\ nm)/Au(2.5\ nm)]_{30}$ were grown on $Si(100)/SiN_x(70\ nm)$ substrates that were thermally isolated from the water-cooled supporting table during deposition. Metallic disks of 99.995% pure elements, with diameter 5 cm, were used as target materials in a high-vacuum Edwards E360A sputtering system with a pair of ATOM-TECH 320-SE planar magnetron sputter sources. All samples were deposited in a cryogenically pumped chamber with base pressure of 2×10^{-7} Torr under an Ar (99.999% pure) pressure of 3 mTorr. An rf magnetron gun operating at 30 W with a deposition rate of 0.07 nm/sec for Co and dc sputtering at 5 W resulting in 0.12 nm/sec of Au were used. It is worth noting that the amorphous SiN_x buffer layer provides an atomically smooth surface where the (111) texture adopted [Fig. 1(b)] by the Co/Au ML's is not induced by the substrate.[9] Five samples were post-annealed separately inside the deposition chamber at 200, 300, 350, 400, and 600 °C for 1 h.

X-ray diffraction (XRD) spectra were collected with a *Siemens* D500 diffractometer in θ-2θ scans, using Cu $K\alpha$ radiation at ambient temperature. Figure 1(a) shows the low-

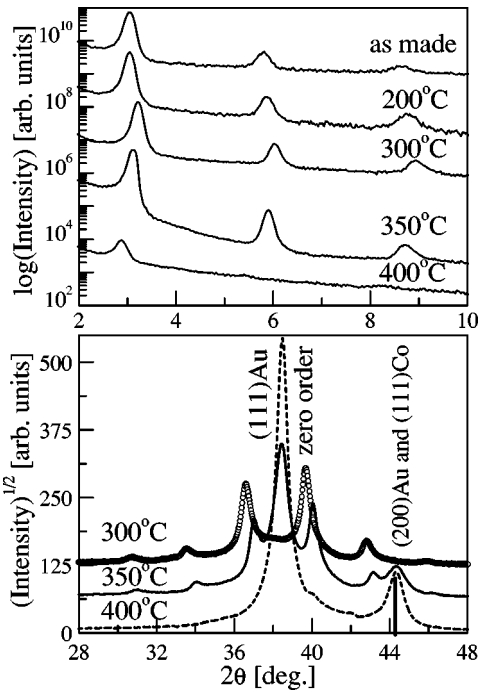

FIG. 1. The temperature evolution of the satellite peaks around the zeroth-order peak from the average lattice is shown at the bottom plot. The low-angle XRD spectra are shown on top.

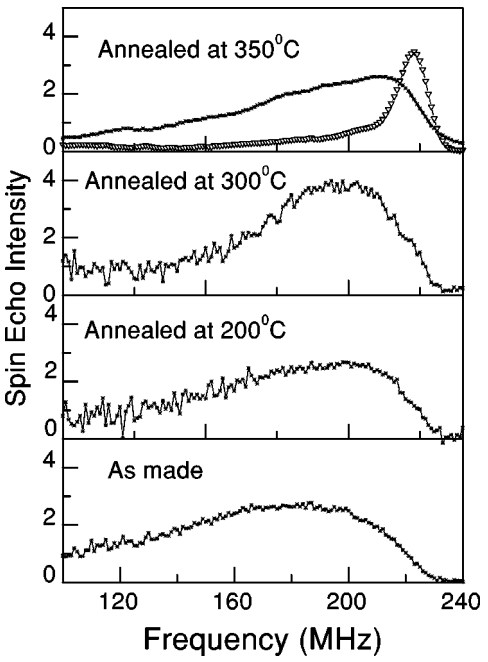

FIG. 2. The spin-echo ^{59}Co NMR spectra, recorded from the as-made sample and from samples annealed at 200, 300, and 350 °C are shown. The 350 °C spectrum is decomposed into a low-T and a high-T (open triangles) subspectrum.

angle superlattice Bragg peaks and Fig. 1(b) shows the grouping of the satellite peaks around the zeroth-order (111) peak, from the average (overall) out-of-plane lattice spacing. The low-angle XRD spectra reveal that the multilayered structure persists up to 400 °C. It is worth mentioning that the XRD spectra (Fig. 1) remain the same for longer post-annealing times (up to 24 h) at 200 and 300 °C. The observed strong intensity of the superlattice peaks after annealing at 200, 300, and 350 °C can be attributed[3] to interface sharpening. The medium-angle spectra show that at 350 °C an extra phase of pure Au coexists with the ML's whereas at 400 °C the layered Co/Au structure is significantly suppressed, exhibiting an almost complete decomposition into Au and Co crystallites. Although the (200) Bragg peak of Au ($d_{200}=0.2038$ nm) cannot be resolved from the (111) peak of fcc Co ($d_{111}=0.2047$ nm) or the (0002) peak of hcp Co ($d_{0002}=0.2023$ nm), the observed peak intensity above 350 °C (centered at $2\theta=44.404°$ or d spacing $=0.2038$ nm) indicates that the diffracted intensity from Co crystallites exhibits a vast peak broadening. Since at 400 °C (Fig. 1) there still exists one low-angle superlattice Bragg peak, it can be argued that the Co layers become discontinuous by forming pancakelike clusters, as in[10] Co/Ag ML's.

Spin-echo ^{59}Co NMR spectra have been recorded at 4.2 K every 1 MHz in the frequency range between 100 and 250 MHz, using a coherent, phase-sensitive spin-echo spectrometer. In magnetic solids the influence of the local structure and symmetry on B_{hf}, the effective hyperfine field sensed by the nuclear spin, arises from two effects: the sensitivity of the transferred hyperfine interaction to the local environment and the dependence of the orbital and atomic dipolar part of B_{hf} on the local symmetry. These features enable one to discriminate between fcc, bcc, and hcp phases, or stacking faults in the pure phase, through the magnitude of B_{hf}, and between fcc, hcp, and trigonal or tetragonal deformed fcc through its anisotropy.[10,11] Furthermore, since the B_{hf} is mainly the result of a delicate balance between the spatial distribution of the spin-up and spin-down electrons, it is also sensitive to distortions of this spatial distributions[12] (strain effects). To obtain the spin-echo intensity that represents the correct hyperfine field distribution and to probe the local magnetic inhomogeneites in a sample, we routinely record the spectra at several values of rf excitations by spanning the range of at least one order of magnitude of the excitation field. This method allows, first, the estimation of an intrinsic enhancement factor that is specific for a given frequency and for which each spectrum must be corrected in order to represent the real hyperfine field distribution, and second, it allows one to separate different magnetic phases[13] if the sample is multiphase.

^{59}Co NMR spectra from the as-made sample and from samples annealed at 200, 300, and 350 °C are shown in Fig. 2. As seen in Fig. 2, annealing up to 300 °C induces only very small changes in the spectral line shapes with respect to the spectrum of the as-made sample. These changes consist in the narrowing of the NMR intensity distribution and the shift of the gravity center of the spectrum, from 167 MHz in the as-made film to 179 MHz for the sample annealed at 300 °C. However, the general profile of these spectra is maintained and, as reported earlier,[8] it is characterized by a broad intensity distribution in a frequency range that is well below the characteristic frequency range of the known crystallographic phases[10,11] of Co.

A dramatic change in the NMR spectrum is observed

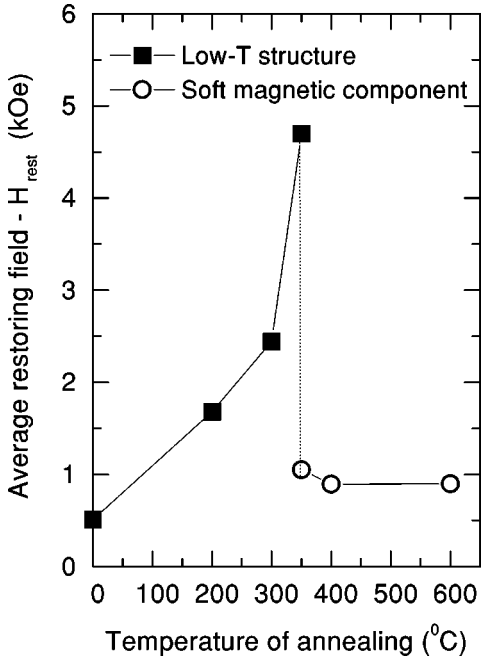

FIG. 3. The average restoring fields, estimated from the low-T and high-T NMR subspectra, are plotted as a function of the annealing temperature. At 350 °C the low-T and high-T components coexist, defining a stiff and a soft magnetic phase, respectively. The lines are guides to the eye.

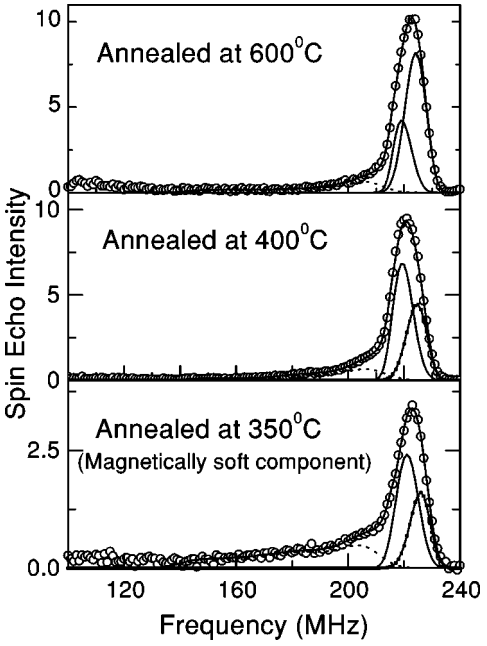

FIG. 4. The NMR spectra of the high-T stucture are shown for the three annealing temperatures of 350, 400, and 600 °C. The observed spin-echo intensity can be fitted with three components, corresponding to the Co/Au interface (dot line), fcc (solid line), and hcp (dashed line) Co structures.

(Fig. 2) after annealing at 350 °C. Both the spectral line shape and its rf power dependence indicate that the multilayer becomes magnetically inhomogeneous. In the NMR experiment such inhomogeneities are detected by the presence of multiple maxima in the signal intensity as a function of the rf field strength. Thus, samples annealed at 200 and 300 °C exhibit only one maximum of the signal intensity at each frequency, whereas the sample that is annealed at 350 °C exhibits two such maxima in the NMR signal intensity, each observed at a different power of the rf excitation pulses. This behavior indicates that there are two ferromagnetic components in the sample, differing considerably in their magnetic stiffness. To separate the NMR subspectra, originating from each component, we have applied a method that is described in Ref. 13. The deconvolution of this spectrum is shown in Fig. 2. Remarkably, the spectrum of the magnetically stiffer component is almost identical with the spectra observed from the samples annealed up to 300 °C. Thus, Co atoms contributing to the intensity of this spectrum must be located in these parts of the Co layer that retain the nanostructure of the as-made multilayer, which we call low-T structure.

Further insight into magnetic inhomogeneity and magnetic stiffness of the studied system can be obtained by introducing the concept of the restoring field[14] ($H_{\rm rest}$), which describes the response of local Co magnetization to external rf field excitations. Thus each value of $H_{\rm rest}$ is determined by the rf field strength that corresponds to a maximum NMR signal and is proportional[14] to magnetic stiffness of the ML's. Now, depending on the source of magnetic stiffness the $H_{\rm rest}$ can be related to the anisotropy field of a single-domain sample, the coercive field resulting from domain wall effects, the exchange biasing or dipolar fields at interfaces, and any combination of these fields. Figure 3 shows that the $H_{\rm rest}$ increases considerably at the initial stages of annealing whereas the low-angle XRD spectra (Fig. 1) show an increase of Co/Au interface sharpness, which is accompanied by the appearance[3] of surface anisotropy due to symmetry breaking. Thus, the observed increase of the average $H_{\rm rest}$ should be interpreted as an enhancement of the interface anisotropy due to the improvement of the Co/Au interface sharpness. Consequently, the steep decrease of $H_{\rm rest}$, which remains constant with annealing temperature at 350 °C and above (open circles in Fig. 3), can be explained by the bridging of Au layers through Co.

Figure 4 shows the subspectrum of the high-T structure at 350 °C together with NMR spectra from samples annealed at 400 and 600 °C, where the subsprectrum of the low-T structure disappears. The observed (Fig. 4) spin-echo intensity can be fitted with three components, centered at the characteristic B_{hf} of Co/Au interface coordination, of fcc and hcp Co structures.[11] The integrated intensities of the fitting lines show that the fraction of hcp-Co stacking increases from 38% in the sample annealed at 350 °C to 69% in the sample annealed at 600 °C. This implies that the shift of B_{hf} upon annealing proceeds by a transition to a structure where hexagonal Co stacking dominates. A plot of the gravity center of each NMR spectrum against the annealing temperature (Fig. 5) shows clearly the separation of the low-T structure from the thermodynamically stable, close-packed structures of Co at 350 °C.

In conclusion, the complementary use of two nondestructive, one macroscopic (XRD) and one microscopic (NMR),

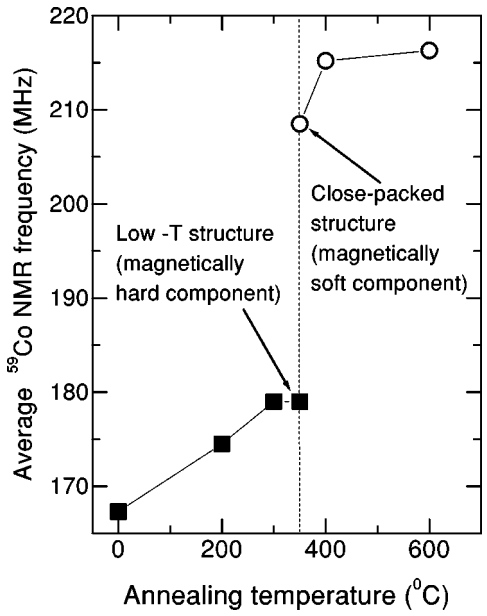

FIG. 5. The gravity center of each NMR spectrum is plotted against the annealing temperature. At 350 °C the low-*T* and high-*T* components coexist, defining two separate gravity centers.

techniques has revealed that polycrystalline $[\mathrm{Co}(1\ \mathrm{nm})/\mathrm{Au}(2.5\ \mathrm{nm})]_{30}$ ML's with (111) texture exhibit two regimes with respect to the microstructural characteristics of Co. In the low-*T* structure, the kinetically grown Co layering is characterized by (i) continuous layers after post-annealing up to 300 °C and (ii) NMR spectra that cannot be assigned to any of the identified structures of Co, indicating the formation of a distorted structure. Post-annealing above 350 °C transforms the low-*T* Co structure and modifies the Co layering into a high-*T* configuration that is characterized by (i) a microstructure that forms a layered granular film due to penetration of Au across the thinner Co layers and (ii) NMR spectra, indicating that inside the pancakelike clusters of Co the lattice adopts the known fcc and hcp structures.

A characteristic of the low-*T* Co structure is that the annealing temperature of ~350 °C, above which our Co/Au ML's (Fig. 4) exhibit the usual NMR spectrum of bulk Co, is comparable with the temperatures where the transformation of bulk hcp Co to fcc stacking occurs (~420 °C) and the amorphous $\mathrm{Co}_{1-x}\mathrm{Au}_x$ thin films decompose[1] into equilibrium Co and Au structures (>300 °C). Thus, besides the fact that the featureless NMR spectrum of the low-*T* nanostructure cannot be assigned to a specific Co coordination,[8,10,11] its thermal stability up to 300 °C and the TEM measurements[9] indicate that an unusual Co nanostructure can be formed when Co layers grow on top of amorphous buffer layers while the substrate temperature is close to room temperature during deposition. Since the only unambiguous evidence for the existence of a metastable Co structure can be given by the crystallographic determination of the specific Co coordination, the importance of these results relies on the fact that makes possible the separation of magnetic inhomogeneites and secondary magnetic phases from complex NMR spectra. To reveal the thermal evolution of the low-*T* Co structure a detailed TEM study is in progress.

This work has been supported by NATO linkage grant HTECH.LG 970571-636(97)JARC-412.

[1] M. Ohring, *The Materials Science of Thin Films* (Academic Press, San Diego, 1992), Sec. 5.7.2, and references therein.
[2] M. Kitada, J. Magn. Magn. Mater. **208**, 244 (2000), and references therein.
[3] F.J.A. den Broeder, D. Kuiper, A.P. van de Mosselaer, and W. Hoving, Phys. Rev. Lett. **60**, 2769 (1988).
[4] C.G. Lee, S.H. Kim, D.H. Lee, and K. Fukamichi, IEEE Trans. Magn. **35**, 2856 (1999).
[5] J. Bernardi, A. Hutten, and G. Thomas, J. Magn. Magn. Mater. **157-158**, 153 (1996).
[6] S. Stavroyiannis, C. Christides, D. Niarchos, Th. Kehagias, Ph. Komninou, and Th. Karakostas, J. Appl. Phys. **84**, 6221 (1998), and references therein.
[7] C. Christides, S. Stavroyiannis, D. Niarchos, M. Gioti, and S. Logothetidis, Phys. Rev. B **60**, 12 239 (1999).
[8] C. Christides, S. Stavroyiannis, D. Niarchos, M. Wojcik, S. Nadolski, and E. Jedryka, Phys. Rev. B **59**, 8812 (1999).
[9] Th. Kehagias, Ph. Komninou, C. Christides, G. Nouet, S. Stavroyiannis, and Th. Karakostas, J. Cryst. Growth **208**, 401 (2000).
[10] E.A.M. van Alphen and W.J.M. de Jonge, Phys. Rev. B **51**, 8182 (1995).
[11] C. Meny, E. Jedryka, and P. Panissod, J. Phys.: Condens. Matter **5**, 1547 (1993).
[12] E.A.M. van Alphen, S.G.E. te Velthuis, H.A.M. de Gronckel, K. Kopinga, and W.J.M. de Jonge, Phys. Rev. B **49**, 17 336 (1994).
[13] M. Malinowska, M. Wojcik, S. Nadolski, E. Jedryka, P. Panissod, C. Meny, M. Knobel, A.D.C. Viegas, and J.E. Schmidt, J. Magn. Magn. Mater. **198-199**, 599 (1999).
[14] P. Panissod, C. Meny, M. Wojcik, and E. Jedryka, in *Magnetic Ultrathin Films, Multilayers and Surfaces—1997*, edited by J. Tobin *et al.*, MRS Symposia Proceedings No. 375 (MRS, Pittsburgh, 1997), p. 157.